Robustness of the subsonic doublet lattice method

L. H. van Zyl
Defence Aeronautics Programme
CSIR
Pretoria, South Africa

ABSTRACT

The subsonic doublet lattice method (DLM) has been the industry standard method for the calculation of unsteady air loads for the past three decades. A recent comparison between the DLM and the subsonic constant pressure panel code ZONA6 suggested that the DLM lacked robustness. However, the DLM code used in the comparison was flawed and not representative of the DLM as such. Results from a contemporary DLM code are presented for the same test cases that were used in the misleading comparison. These new results show that the DLM can produce valid results for all the test cases considered. Where feasible, a comparison is made between results from the present DLM code and the published ZONA6 results.

NOMENCLATURE

$C_{L\alpha}$	lift coefficient slope
$C_{M\alpha}$	moment coefficient slope
C_p	pressure coefficient
k	reduced frequency based on full chord
M	Mach number
N_x, N_y	number of chordwise and spanwise panels, respectively
U	freestream velocity
ω	circular frequency

1.0 INTRODUCTION

The subsonic doublet lattice method (DLM)[1-5] has been a popular method for calculating unsteady air loads for the aeroelastic analysis of general configurations for the past three decades. Several enhancements were introduced during this period, including the improved treatment of near-coplanar surfaces[2] and increased integration accuracy[3]. All the results presented here were calculated using a DLM code which incorporates the improvements of Refs 2 and 3. All calculations were however repeated using a code which does not incorporate the quartic approximation to the kernel numerator of Ref. 3, and the differences are discussed.

The DLM can be regarded as an extension of the vortex lattice method (VLM), which is used for steady load calculation. The downwash factors are calculated as the sum of the steady component, identical to that of the VLM, and an unsteady component. In the calculation of the unsteady component the kernel numerators are approximated by polynomials and the resulting expression integrated analytically. In steady flow the DLM reverts to the VLM.
The unsteady planar downwash factor is given in Ref. 2 as;

$$D_{1rs} = \frac{\Delta x_s}{8\pi}\int_{-e}^{e}\frac{\{K_1 \exp[-i\omega(\bar{x}-\bar{\eta}Tan\lambda_s)/U]-K_{10}\}T_1}{r_1^2}\mathrm{d}\bar{\eta} \quad \ldots (1)$$

where the symbols have the meanings as defined in Ref. 2 This integral cannot be solved analytically and is evaluated by making a polynomial approximation to the numerator of the integrand and integrating the resulting expression analytically.

$$D_{1rs} \approx \frac{\Delta x_s}{8\pi}\int_{-e}^{e}\frac{P_1(\bar{\eta})}{(\bar{y}-\bar{\eta})^2+\bar{z}^2}\mathrm{d}\bar{\eta} \quad \ldots (2)$$

where;

$$P_1(\bar{\eta}) = A_1\bar{\eta}^2 + B_1\bar{\eta} + C_1 \quad \ldots (3)$$

Paper No. 2716. Manuscript received 22 August 2001, revised version received 18 December 2002, accepted 1 February 2003.

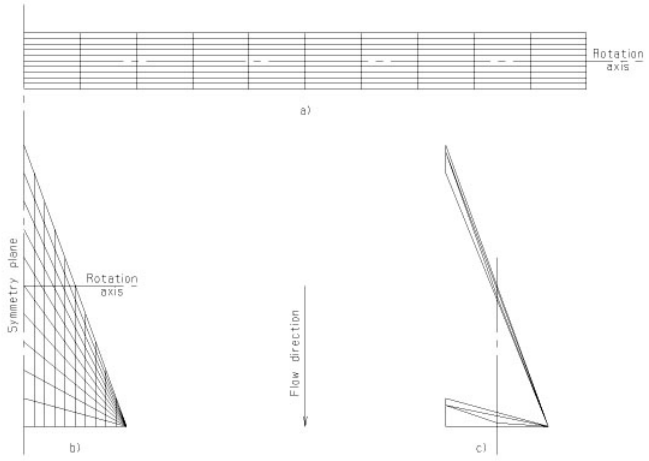

Figure 1. Planform and panelling of wings analysed: (a) *AR* 20 rectangular wing, (b) 70° delta wing, (c) geometry of leading and trailing boxes of the outboard strip of the delta wing.

in the case of the parabolic approximation of Ref. 2. In Ref. 3 the parabolic approximation is replaced by a quartic approximation of the form;

$$Q_1(\bar{\eta}) = A_1\bar{\eta}^2 + B_1\bar{\eta} + C_1 + D_1\bar{\eta}^3 + E_1\bar{\eta}^4 \qquad \ldots (4)$$

The accuracy of the unsteady downwash factor depends on the accuracy of the approximation to the kernel numerator. In order to maintain accuracy a limit has been set on the maximum box aspect ratio that may be used. There is also a requirement for a minimum number of chordwise and spanwise panels required to achieve convergence of the pressure distribution. The requirement for the number of chordwise boxes is expressed as the number of boxes per wavelength of the unsteady wake disturbance, $2\pi U/\omega$. The requirement for the number of spanwise strips has not been investigated separately since the combination of the minimum number of chordwise boxes and the maximum box aspect ratio implies a minimum number of spanwise strips . The published guidelines have not been consistent, however, the limits reported in Ref. 4 are generally accepted.

In any VLM code a limiting expression of the vortex formula must be used for the calculation of the bound vortex contribution to the downwash at a point on or close to the extension of a bound vortex. The criterion for using the limiting expression is not discussed in Ref. 2. One possibility is to use the limiting expression when the angle between the bound vortex and a line from the collocation point to a vortex endpoint is small. If this criterion is applied carelessly, it may cause the limiting expression to be erroneously used in the calculation of the downwash at a box's own collocation point. It is believed that an error of this kind affected the DLM results of Liu, Chen, Yao and Sarhaddi[6] in their comparison between the DLM and their subsonic constant pressure panel code ZONA6[7]. The present work aims to confirm the robustness of the DLM by providing proper results for the same test cases that were used to draw its robustness into question.

The first test case of Liu *et al* was that of an *AR* 20 rectangular wing pitching about its midchord at M = 0·0. Their DLM results for this case were not affected by the error in their DLM code and are representative of the DLM with a parabolic approximation to the kernel numerators. The improvement in the results presented here is due to the increased accuracy of a quartic approximation over a parabolic approximation.

Their second test case was that of a series of slender delta wings at a steady angle-of-attack at M = 0·8. This case only tests the VLM part of the code and their DLM results were affected by the error in their DLM code. The present DLM results show much improved convergence to the slender wing limit.

Their third test case was that of a 70° delta wing pitching about its root midchord at reduced frequencies k = 0·0, 0·5 and 10·0, and M = 0·8. The DLM results presented by Liu *et al* for almost all cases were invalid, because of the error in their DLM code. In particular, the k = 0·0 case shows a failure of the VLM part of their DLM code. This should have pointed to an error in their DLM code, but was used instead to argue that the DLM formulation lacks robustness[6].

2.0 MODELLING

Figure 1 shows the planform and panelling of the *AR* 20 rectangular wing and the 70° delta wing. In both cases the coarsest panelling scheme that was analysed, is shown. Symmetric half models were used in all cases and the numbers of spanwise strips quoted are the numbers of spanwise strips in the half models.

The existing modelling guidelines for the DLM were violated in many of the cases presented by Liu *et al* In the case of the rectangular wing with $N_x \times N_y = 10 \times 10$ the box aspect ratio is ten. In the case of the 70° delta wing with $N_x = 10$ the aspect ratios of the boxes in the outboard strip is 7·28 and with $N_x = 40$ it is 29·1. Reference 4 quotes a limit of three for the earlier DLM formulation of Ref. 2 and six to ten for the new DLM formulation of Ref. 3.

There are 6·28 chordwise boxes per wavelength in the case of the *AR* 20 rectangular wing as well as at the root of the 70° delta wing at k = 10 and N_x = 10. Reference 4 quotes a minimum number of chordwise boxes per wavelength of 12 to 25 for the earlier formulation of Ref. 2 and (50 for the new formulation of Ref. 3.

The existing box aspect ratio limitation may be unnecessarily limiting. It is practically impossible to obtain a worse result by refining the chordwise panelling and this is illustrated in the present results for the 70° delta wing where the 10 × 400 panelling scheme results in a box aspect ratio in the outboard strip of 291. The box aspect ratio limit should rather be formulated as a number of spanwise strips per wavelength. Applying the existing requirements for the number of chordwise boxes per wavelength and box aspect ratio simultaneously would result in eight (≈25/3) spanwise strips per wavelength for the earlier formulation of Ref. 2, and six (≈50/8) spanwise strips per wavelength for the new formulation of Ref. 3.

The geometry of the leading and trailing boxes of the outboard strip of the 70° delta wing with ten chordwise boxes is shown in Fig. 1. The bound vortices as well as lines from the vortex endpoints to the collocation points are shown. The angles between the bound vortex and the lines from the left and right endpoints of the bound vortex to the collocation point are 55′ and 1°, respectively, for the leading box and 7°19′ and 7°42′, respectively, for the trailing box. It is seen that a large sweep angle, along with a high box aspect ratio, causes the angle between the bound vortex and a line from a bound vortex endpoint to the collocation point to become small. These small angles make the results susceptible to coding errors of the kind described earlier.

3.0 RESULTS

3.1 Rectangular wing of *AR* = 20

Figure 2 presents the lift coefficient slope versus reduced frequency k for the rectangular wing pitching about its midchord. These results were calculated using the same two panelling schemes as those used by Liu *et al*[6], *viz*. $N_x \times N_y = 10 \times 10$ and $N \times N_y = 10 \times 40$. In addition an estimate of the fully converged solution[8], extrapolated from results of the present DLM for a 20 × 20 and a 40 × 40 panelling scheme is shown. The present DLM results are compared also to Theodorsen's two-dimensional theory[9]. However, a small

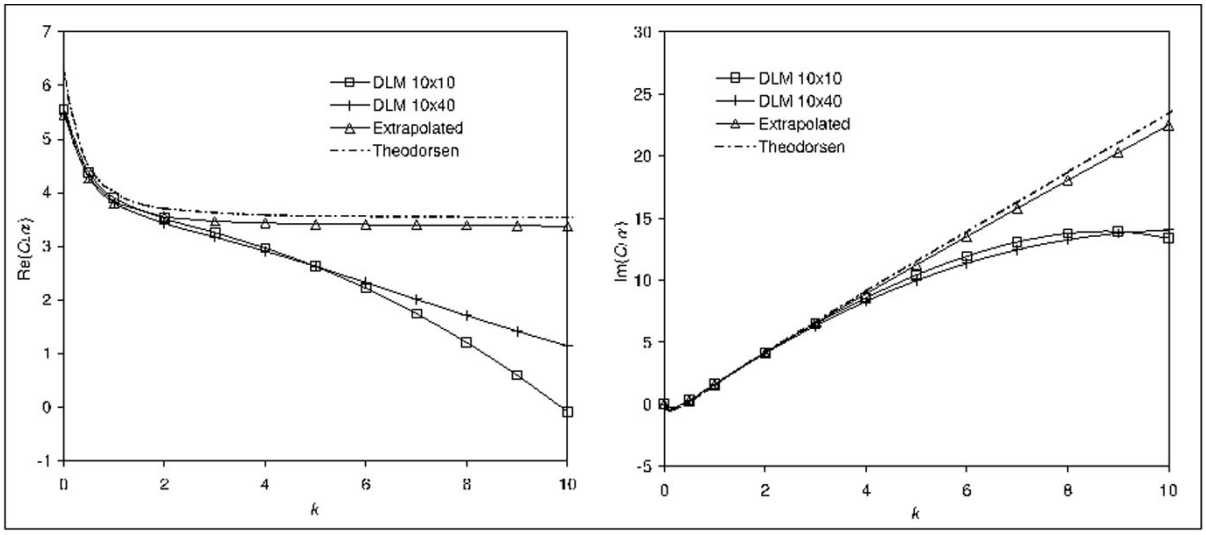

Figure 2. $C_{L\alpha}$ *versus* reduced frequency of the *AR* 20 rectangular wing pitching about its midchord.

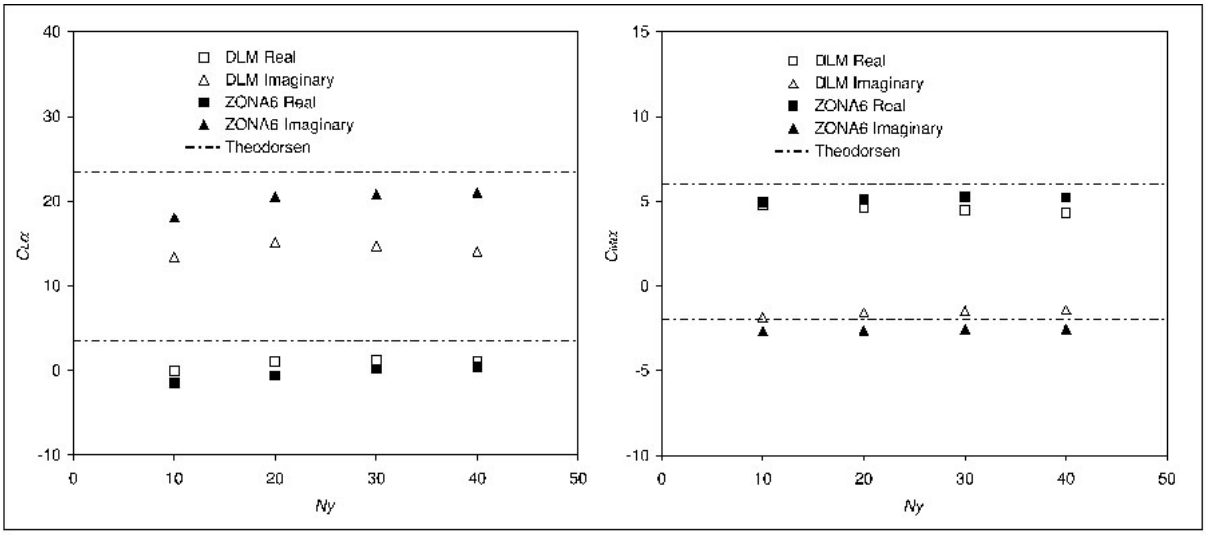

Figure 3. Effect of the number of spanwise panels on $C_{L\alpha}$ and $C_{M\alpha}$ of the *AR* 20 rectangular wing pitching about its midchord at $k = 10{\cdot}0$.

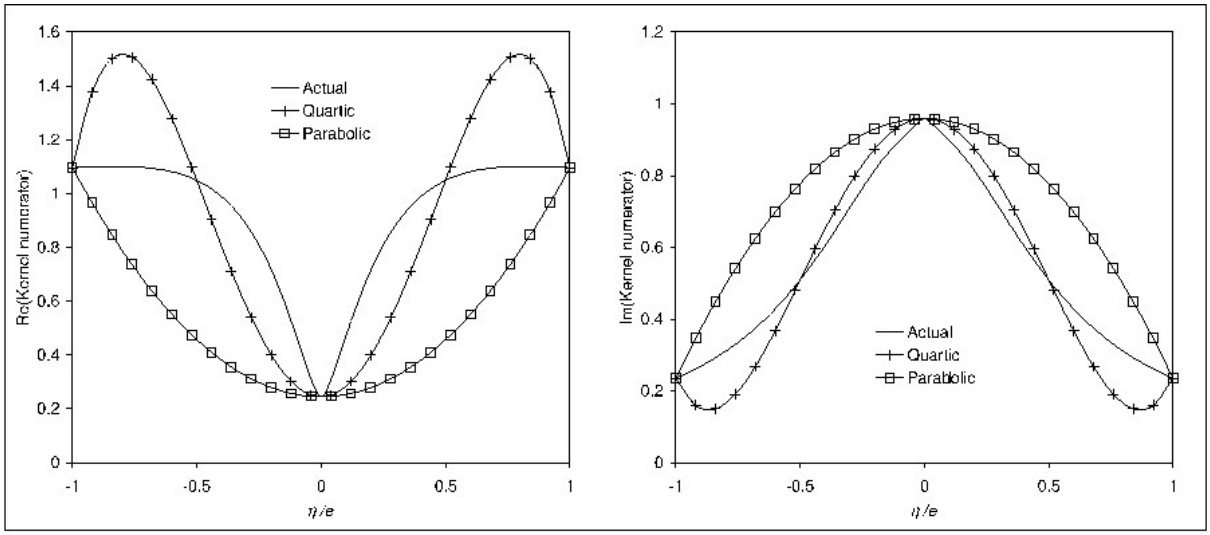

Figure 4. Parabolic and quartic approximations to the kernel numerator.

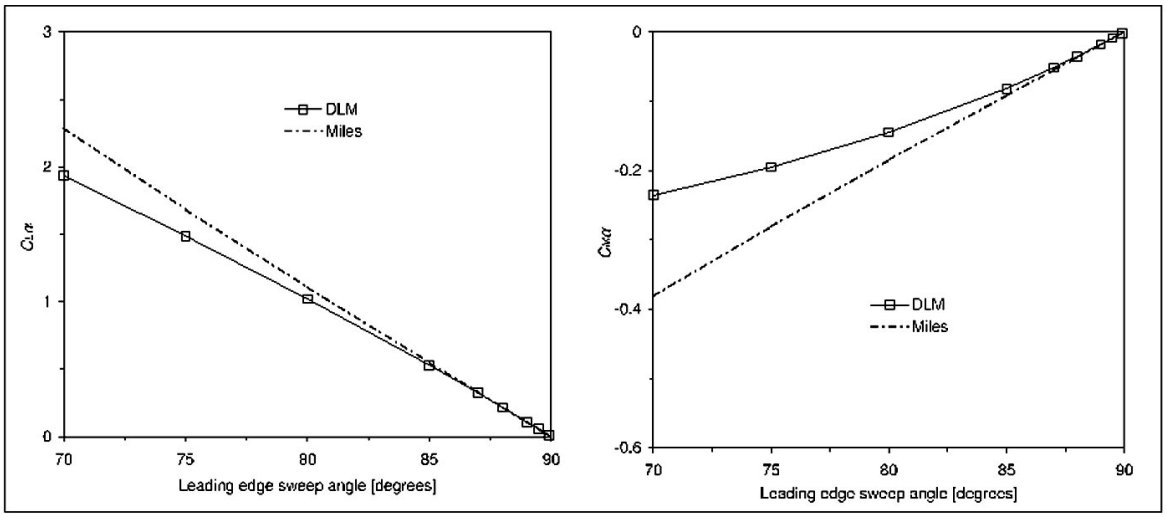

Figure 5. Effect of sweepback angle on $C_{L\alpha}$ and $C_{M\alpha}$ of a slender delta wing.

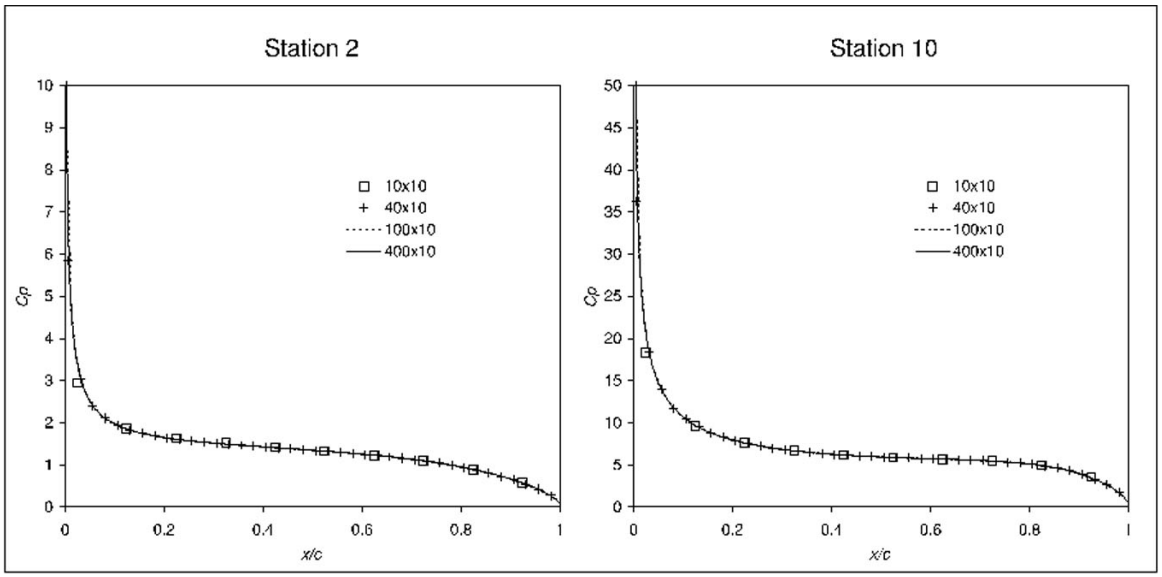

Figure 6. Pressures on two spanwise stations of the 70° delta wing at incidence.

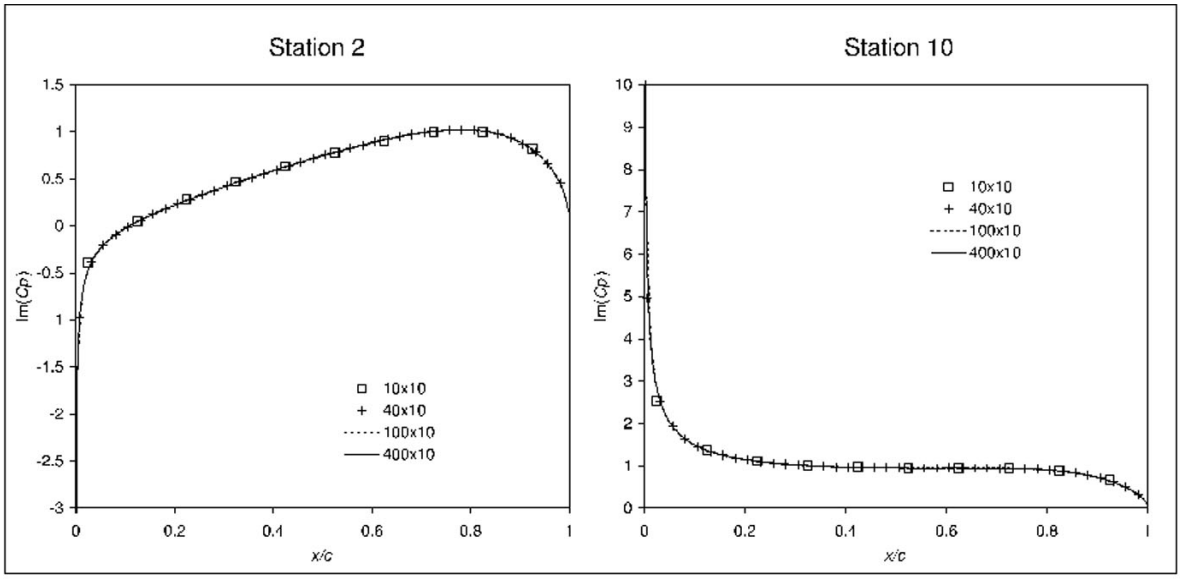

Figure 7. Out of phase pressures on two spanwise stations of the 70° delta wing pitching about its root midchord at $k = 0{\cdot}5$.

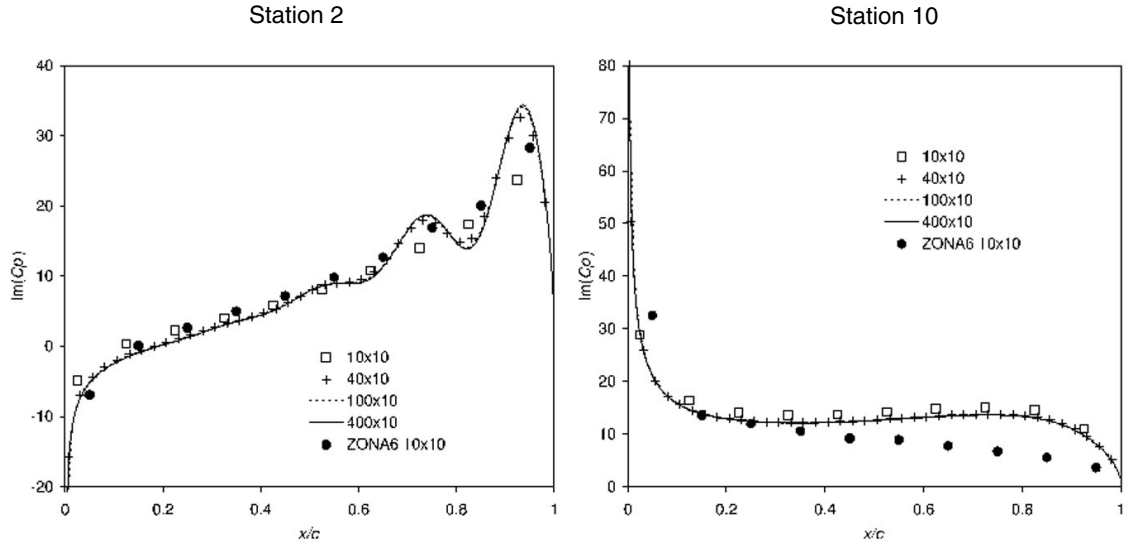

Figure 8. Out of phase pressures on two spanwise stations of the 70° delta wing pitching about its root midchord at $k = 10{\cdot}0$.

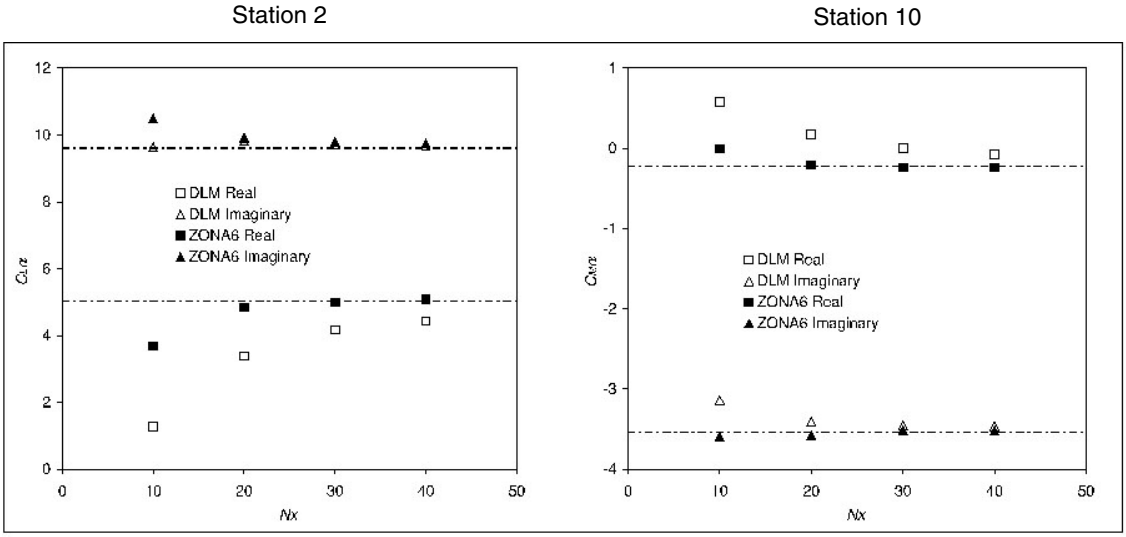

Figure 9. Effect of the number of chordwise panels on $C_{L\alpha}$ and $C_{M\alpha}$ of the 70° delta wing pitching about its root midchord at $k = 10{\cdot}0$.

difference is to be expected because of the finite aspect ratio of the wing. The present DLM results for the 10 × 40 panelling scheme are similar to those presented by Liu *et al*. The present DLM results for the 10 × 10 panelling scheme are much closer to the theoretical result and to the results for the 10 × 40 panelling scheme than was found by Liu *et al*. The estimated fully converged results closely follow the theoretical results.

Figure 3 presents the lift coefficient slope and moment coefficient slope at $k = 10{\cdot}0$ for panelling schemes with different numbers of spanwise strips and 10 chordwise boxes. Liu *et al* found that their DLM results for the 10 × 10 panelling scheme deviated substantially from the general trend whereas the present DLM results for the 10 × 10 panelling scheme fit in with the general trend. The ZONA6 results shown here were digitised from Ref. 6, but should be sufficiently accurate to compare the results of the ZONA6 code and the present DLM code. The results are similar except for the imaginary part of the lift coefficient slope, where the ZONA6 results are significantly closer to the theoretical value.

The DLM code used by Liu *et al* probably did not implement the improved integration scheme of Rodden, Taylor and McIntosh[3]. The present DLM code was degraded to the earlier integration scheme and the calculations were repeated. The results closely matched the DLM results presented by Liu *et al*. The improvement in the DLM results presented here over those presented by Liu *et al* is, therefore, entirely due to the increased accuracy of a quartic approximation over a parabolic approximation.

The parabolic and quartic approximations to the kernel numerator are compared in Fig. 4 for the unsteady downwash of a box of the AR 20 wing with a 10 × 10 panelling scheme at $k = 10{\cdot}0$ at its own collocation point. Neither approximation is particularly good, however, the quartic approximation is in error in one sense over half the range and in the other sense over the other half, whereas the parabolic approximation is in error in one sense over the entire range.

3.2 Slender delta wings

The comparison between Miles's slender wing theory[10] and the present DLM results for a 10 × 10 panelzling scheme is shown in Fig. 5. Contrary to the Liu *et al* DLM results, the present DLM

results approach the slender wing results from one side as the leading edge sweep angle is increased up to 89°. The present DLM results for $C_{L\alpha}$ then cross over the slender wing results and the difference increases to 0·1% at 89·95°. The present DLM results for CMa do not cross over the slender wing results and the difference decreases from 2% at 89° to 1% at 89·95°. In contrast the ZONA6 results presented by Liu *et al* cross over the slender wing results between 75° and 85°. No indication is given of how the ZONA6 results compare to the slender wing theory at leading edge sweep angles greater than 85°.

In an earlier study of the application of the DLM to delta wings[11], it was found that the estimate for the fully converged DLM solution approached the slender wing limit from one side for leading edge sweep angles up to 89·95°, at which point the difference between the slender wing limit and the estimate of the fully converged DLM result was 0·02% in both $C_{L\alpha}$ and $C_{M\alpha}$. It would therefore seem that the present DLM results for the 10 × 10 panelling scheme are closer to the correct results than the ZONA6 results at large leading edge sweep angles.

3.3 70° delta wing

Figure 6 presents the pressure distributions over the second and tenth spanwise stations of the 70° delta wing at a steady angle of attack at M = 0·8. Results for 10 × 10, 40 × 10, 100 × 10 and 400 × 10 (N_x × N_y) panelling schemes are shown and the C_p values are normalised with the angle of attack. The box aspect ratio of the boxes in the outboard spanwise strip is 291 in the case of the 400 × 10 panelling scheme and no adverse effect of the large box aspect ratio is evident. In contrast to the DLM results presented by Liu *et al*, the present DLM results are smooth and convergence is acceptable from the 10 × 10 panelling scheme.

Figure 7 presents the out-of-phase pressure distributions over the second and tenth spanwise stations of the 70° delta wing pitching about its root midchord at k = 0·5. The same observations as for the steady case apply.

Figure 8 presents the out-of-phase pressures distributions over the second and tenth spanwise stations of the 70° delta wing pitching about its root midchord at k = 10·0. The pressure distributions are still smooth, however, at least 40 chordwise boxes are needed for acceptable convergence. The pressure distributions from the ZONA6 constant pressure panel code for the 10 × 10 panelling scheme were digitised from Ref. 6 and are also shown on the figure. There are significant differences between the pressure distributions from the present DLM code and those from the ZONA6 code.

The results for the 70° delta wing test cases were also calculated using the parabolic approximation to the kernel numerators. The results were not significantly different from the results presented here for the quartic approximation.

Figure 9 presents the lift coefficient slope and moment coefficient slope for the 70° delta wing pitching about its root midchord at k = 10·0 and M = 0·8 for panelling schemes with different numbers of chordwise boxes and ten spanwise strips. The results are compared to an estimate of the fully converged result, extrapolated from results of the present DLM code for a 20 × 20 and a 40 × 40 panelling scheme. Liu *et al* found irregular trends in their DLM results, whereas the present DLM results show more regular trends. The ZONA6 results shown here were digitised from Ref. 6 and are generally closer to the estimate of the fully converged results than the present DLM results.

4.0 CONCLUSIONS

The present results confirm the robustness of the DLM. Neither large sweep angles nor large panel aspect ratios caused the method to fail. The accuracy of the approximation to the kernel numerators was found to have a significant effect in cases where the panel size is large compared to the wavelength.

A limited comparison with ZONA6 results indicates that for a given panelling scheme ZONA6 can be expected to produce results closer to the fully converged solution than the present DLM. It is not apparent why this should be so because the ZONA6 code is an oscillatory extension of the Woodward constant pressure method for steady flow[12]. Assuming a constant pressure on a panel (box) is a crude approximation that should require very small boxes, both spanwise (depending on the wing aspect ratio) and chordwise (depending on the reduced frequency). No guidelines for idealisation have been proposed as a function of aspect ratio, reduced frequency and Mach number. Furthermore, there is a downwash collocation point on the centreline of the box whose location is never discussed. Woodward suggested 95% of the box chord although 85% is used in ZONA6. The sensitivity of results to this choice has never been published.

The present DLM code is not a commercial code, however, it is available for free from the author to anyone wishing to repeat the calculations or to inspect the code.

REFERENCES

1. ALBANO, E. and RODDEN, W.P. A doublet-lattice method for calculating lift distributions on oscillating surfaces in subsonic flows, *AIAA J*, 1969, **7**, (2), pp 279-285.
2. RODDEN, W.P., GIESING, J.P. and KALMAN, T.P. New developments and applications of the subsonic doublet-lattice method for nonplanar configurations, AGARD Conference Proceedings, CP-80-71, Part II, No 4, 1971.
3. RODDEN, W.P., TAYLOR, P.F. and MCINTOSH, S.C. Further refinement of the nonplanar aspects of the subsonic doublet-lattice lifting surface method, ICAS Conference Proceedings, Paper 96-2.8.2, 1996.
4. RODDEN, W.P., TAYLOR, P.F., MCINTOSH, S.C. and BAKER, M.L. Further convergence studies of the enhanced subsonic doublet-lattice oscillatory lifting surface method, International Forum on Aeroelasticity and Structural Dynamics, Rome, June 1997.
5. RODDEN, W.P. The development of the doublet-lattice method, International Forum on Aeroelasticity and Structural Dynamics, Rome, June 1997.
6. LIU, D.D., CHEN, P.C., YAO, Z.X. and SARHADDI, D. Recent advances in lifting surface methods, *Aeronaut J*, October 1996, **100**, (998), pp 327-339.
7. CHEN, P.C., LEE, H.W. and LIU, D.D. Unsteady subsonic aerodynamics for bodies and wings with external stores including wake effect, *J Aircr*, 1993, **30**, (5), pp 618-628.
8. VAN ZYL, L.H. Convergence of the subsonic doublet lattice method, *J Aircr*, 1998, **35**, (6), pp 977-979.
9. THEODORSEN, T. General theory of aerodynamic instability and the mechanism of flutter, NACA Report No 496, 1935.
10. MILES, J.W. *Potential Theory of Unsteady Supersonic Flow*, Cambridge University Press, 1959.
11. VAN ZYL, L.H. Application of the subsonic doublet lattice method to delta wings, *J Aircr*, 1998, **36**, (3), pp 609-610.
12. WOODWARD, F.A. An improved method for the aerodynamic analysis of wing-body-tail configurations in subsonic and supersonic flow, NASA CR-2228, 1973.